Hong Kong J Radiol. 2023;26:6-13 | https://doi.org/10.12809/hkjr2317503

ORIGINAL ARTICLE **CME**

Diagnostic Accuracy of ^{18}F-Fluorodeoxyglucose Positron Emission Tomography/Computed Tomography in Preoperative Mediastinal/ Extramediastinal Nodal Staging of Non–Small-Cell Lung Carcinoma

KS Ng, KK Ng, KS Chu, BT Kung, TK Au Yong

Nuclear Medicine Unit and Clinical PET Centre, Queen Elizabeth Hospital, Hong Kong

ABSTRACT

Introduction: *Lung cancer has the highest incidence and mortality among malignancies in many countries. ^{18}F-Fluorodeoxyglucose (^{18}F-FDG) positron emission tomography/computed tomography (PET/CT) is commonly indicated for the preoperative nodal staging of non–small-cell lung carcinoma. While maximum standardised uptake value (SUV_{max}), visual scoring systems and nodal diameter have been proposed to distinguish benign from malignant nodes, studies comparing the different measurements have been limited. Correct nodal staging is crucial in determining if treatment intent is curative or palliative. This study aimed to evaluate the accuracies of nodal staging in ^{18}F-FDG PET/CT based on different methods.*

Methods: *A total of 467 mediastinal/extramediastinal lymph nodes from 97 patients, who underwent staging ^{18}F-FDG PET/CT at our centre for non–small-cell lung carcinoma, were retrospectively reviewed. The nodes were evaluated based on SUV_{max}, five-point visual interpretation score, and diameter. Their sensitivities, specificities and accuracies were compared with histology using receiver operating characteristics curves and areas under the curves (AUCs). Subgroup analyses based on T staging, histology, epidermal growth factor receptor (EGFR) status, lymph node locations, and tumour SUV_{max} were also investigated.*

Results: *The diagnostic performance of visual score (at optimal cut-off of 3) yielded the highest specificity (0.932), accuracy (0.916), positive predictive value (0.623), and negative predictive value (0.972), results of which were similar to SUV_{max} of 2.5 and better than nodal diameter of 10 mm. Subgroup analyses showed that visual interpretation achieved satisfactory AUCs in different T stages, histologies, EGFR statuses, locations of lymph nodes, and tumour $SUVs_{max}$.*

Conclusion: *The five-point visual interpretation is a convenient diagnostic tool with performance better than nodal diameter, and similar to that of SUV_{max}.*

Key Words: *Carcinoma, non–small-cell lung; Fluorodeoxyglucose F18; Lung neoplasms; Mediastinum; Positron emission tomography computed tomography*

Correspondence: *Dr KS Ng, Nuclear Medicine Unit and Clinical PET Centre, Queen Elizabeth Hospital, Hong Kong*
Email: nks176@ha.org.hk

Submitted: 18 Nov 2021; Accepted: 1 Apr 2022.

Contributors: All authors designed the study, acquired the data, analysed the data, drafted the manuscript, and critically revised the manuscript for important intellectual content. All authors had full access to the data, contributed to the study, approved the final version for publication, and take responsibility for its accuracy and integrity.

Conflicts of Interest: As editors of the journal, KSN and TKAY were not involved in the peer review process. Other authors have disclosed no conflicts of interest.

Funding/Support: This research received no specific grant from any funding agency in the public, commercial, or not-for-profit sectors.

Data Availability: All data generated or analysed during the present study are available from the corresponding author on reasonable request.

Ethics Approval: This study was approved by the Research Ethics Committee (Kowloon Central/Kowloon East Cluster) of Hospital Authority, Hong Kong (Ref No.: KC/KE-19-0048-ER-4). Informed consent was waived because of the retrospective nature of the study.

中文摘要

^{18}F-氟脫氧葡萄糖正電子／電腦斷層掃描在非小細胞肺癌術前縱隔／縱隔外淋巴結分期中的診斷準確性

吳國勝、吳官橋、朱競新、龔本霆、歐陽定勤

簡介：肺癌在許多國家的惡性腫瘤中發病率和死亡率最高。^{18}F-氟脫氧葡萄糖（^{18}F-FDG）正電子發射斷層掃描／計算機斷層掃描（PET/CT）通常用於非小細胞肺癌的術前淋巴結分期。雖然已提出最大標準化攝取值（SUV_{max}）、視覺評分系統和淋巴結直徑來區分良性和惡性淋巴結，但比較不同測量值的研究不多。正確的淋巴結分期對於確定治療目的是治愈性還是姑息性至關重要。本研究旨在評估基於不同方法的^{18}F-FDG PET/CT淋巴結分期的準確性。

方法：本研究回顧性分析在本中心進行^{18}F-FDG PET/CT分期的非小細胞肺癌患者97例共467個縱隔／縱隔外淋巴結。淋巴結根據SUV_{max}、五級視覺判讀分數和直徑進行評估。我們使用接受者操作特徵曲線和曲線下面積（AUC）將它們的敏感性、特異性和準確性與組織學比較，並研究基於T分期、組織學、表皮生長因子受體（EGFR）狀態、淋巴結位置和腫瘤SUV_{max}的亞組分析。

結果：視覺分數（最佳截斷值為3）的診斷性能獲得最高特異性（0.932）、準確性（0.916）、陽性預測值（0.623）及陰性預測值（0.972），結果與SUV_{max}值2.5的結果相似，以及優於淋巴結直徑10 mm的結果。亞組分析顯示，視覺解釋在不同的T分期、組織學、EGFR狀態、淋巴結位置和腫瘤SUV_{max}中達到滿意的AUC。

結論：五級視覺判讀是一種方便的診斷工具，性能優於淋巴結直徑，並與SUV_{max}相似。

INTRODUCTION

In many countries, lung cancer has the highest incidence and mortality among all malignancies.[1] Mediastinal/extramediastinal nodal status is the most important factor determining the management of early non–small-cell lung carcinoma (NSCLC). For N0 or N1 disease, according to the 7th and 8th editions of American Joint Committee on Cancer staging,[2,3] curative surgical resection can be offered.[4] For N2 (subcarinal or ipsilateral mediastinal metastasis) disease, the usual treatment is chemoradiotherapy (CRT).[4] Accurate mediastinal nodal staging is critical but challenging. Whereas mediastinoscopy is the gold standard, this invasive procedure carries 0.5% life-threatening risks of major complications including arrhythmia, respiratory failure, and infection.[5] Although staging with computed tomography based on nodal diameter is non-invasive, it has limited accuracy.[6,7] ^{18}F-fluorodeoxyglucose (^{18}F-FDG) positron emission tomography/computed tomography (PET/CT) is useful in NSCLC staging.[8-11] Both semiquantitative assessment and qualitative visual interpretation are recommended for distinguishing benign from malignant lymph nodes (LNs).[10-14] In a semiquantitative approach, the maximum standardised uptake value (SUV_{max}) is used.[10-12] Yet, SUV_{max} depends on many physiological as well as technical factors, such as injection time, uptake period, and blood glucose level.[15,16] Thus, absolute SUV_{max} is difficult to compare between different PET/CT systems or subjects. Studies have compared the accuracies of simple SUV_{max} and visual score generated by different comparisons with the activity in the aorta and other locations, as well as with a simple unified windowing technique.[13,14] We aimed to evaluate the performance of ^{18}F-FDG PET/CT on mediastinal/extramediastinal nodal staging of NSCLC based on SUV_{max}, visual score, and nodal diameter. The disparity between radiological and pathological staging was also reviewed.

METHODS

Case Enrolment

Cases of newly diagnosed lung cancer patients who underwent whole-body ^{18}F-FDG PET/CT for staging in our centre at Queen Elizabeth Hospital from 1 January 2016 to 31 December 2016 were retrospectively analysed. Cases were included only if they had (1) histological

evidence of primary NSCLC and (2) histological mediastinal/extramediastinal LN staging. Cases were excluded if (1) the time interval between PET/CT and histological LN examination was >2 months, or (2) treatment was started before PET/CT.

Technical Aspects

All PET/CT examinations were acquired with a Discovery 710 (General Electric, Milwaukee [WI], US) according to the 2010 procedural protocol of the European Association of Nuclear Medicine for oncological PET imaging.[17] The mean ^{18}F-FDG activity administrated was 370 ± 44.4 MBq. After a mean uptake time of 60 minutes (standard deviation = 6.24), image data were acquired from the skull vertex to the mid-thighs in 7 to 8 bed positions (3 minutes per bed position) with mean axial bed coverage of 15.2 cm per bed and 9 sections bed overlap in the 2-dimensional acquisition mode. Reconstruction using optimisation of ordered subset expectation maximisation was performed with 4.2 mm section thickness in a 128 × 128 matrix and processed through a standard filter. Non-contrast CT was acquired for anatomical correlation and attenuation correction with the following parameters: 120 mA tube current, 140 kV tube voltage, 0.8 s gantry rotation speed, 0.75 pitch, 0.5 mm section thickness and 512 × 512 matrix. The mean blood glucose level was 5.5 mmol/L (standard deviation = 0.91).

Positron Emission Tomography/Computed Tomography Interpretation

This study evaluated the accuracy of staging PET/CT in the diagnosis of mediastinal/extramediastinal LNs. A nuclear medicine physician, blinded to the patients' clinical background and histological results, assessed the PET/CT images according to the Mountain and Dresler nodal station scheme[18] with an Advantage Workstation Volume Viewer 4.7 (General Electric, Milwaukee [WI], US). If the histologically evaluated LNs were identifiable on PET/CT, three nodal features were analysed: SUV_{max}, visual score (as illustrated below) and diameter (short axis in axial plane). SUV is defined as the activity measured in a volume of interest divided by the injected ^{18}F-FDG dose, based on body weight:

$$SUV = \frac{Activity_{VOI}\,(MBq/mL)}{Dose_{injected}\,(MBq/kg)}$$

A five-point visual score of LNs was used, with a standardised lower threshold set at 0 and the upper threshold at 2 times the liver's mean standardised uptake value (SUV_{mean}).[14] The LNs were rated based on the maximum intensity projection image with grey scale images (Figure 1):

- Score 0: No LN uptake
- Score 1: LN uptake < mediastinal blood pool
- Score 2: mediastinal blood pool ≤ LN uptake < SUV_{mean} of liver
- Score 3: SUV_{mean} of liver ≤ LN uptake <2 × SUV_{mean} of liver
- Score 4: LN uptake ≥2 × SUV_{mean} of liver

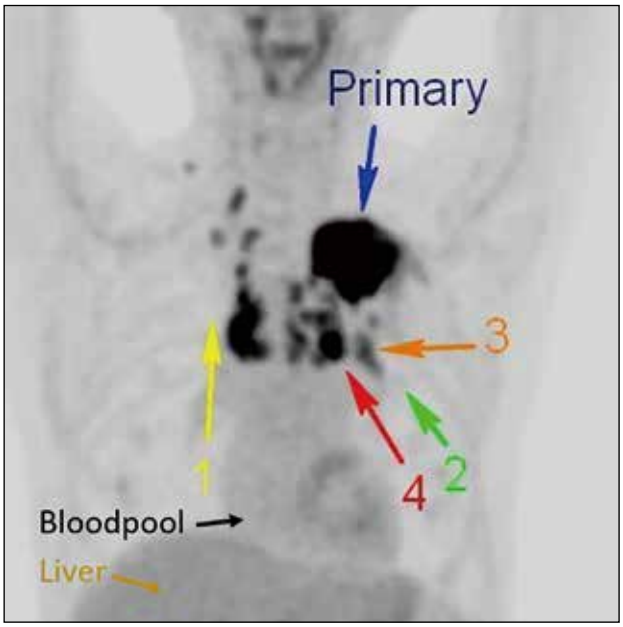

Figure 1. Representative maximum intensity projection for visual scores of 1 to 4, with bloodpool, liver, and primary tumour labelled (arrows).

For primary tumour with uptake similar to that of liver, the respective LNs were scored 4 if their uptakes were similar to the uptake of the primary.[14] If a LN was evaluated histologically but unidentifiable on PET/CT, a score of 0 was assigned and a 2-cm sphere was marked as a volume of interest in the corresponding anatomical location for SUV_{max}.

Histological Evaluation

Mediastinal/extramediastinal LNs were sampled by cardiothoracic surgeons or respiratory physicians via lobectomy (59%), mediastinoscopy (14%), video-assisted thoracoscopic surgery (11%), endobronchial ultrasound (8%), pneumonectomy (5%) or wedge resection (3%). Anatomical staging was evaluated by pathologists according to Mountain and Dresler scheme.[18]

Statistical Analysis

Statistical analysis was performed using SPSS (Window version 20.0; IBM Corp, Armonk [NY], US). Receiver operating characteristics (ROC) curves as well as corresponding areas under the curve (AUCs) based on SUV_{max}, visual score, and nodal diameter were compared. The optimal cut-off to distinguish benign from malignant LNs in PET/CT is the minimum of $\sqrt{(1-specificity)^2 + (1-sensitivity)^2}$. The respective sensitivities, specificities, accuracies, false negative and positive values were determined. Subgroup analyses were also examined according to primary tumour T stage (T1-2 vs. T3-4), histology (adenocarcinoma vs. squamous cell carcinoma), epidermal growth factor receptor (EGFR) status (wild type vs. mutated), primary tumour SUV_{max} (<10 vs. ≥10), and LN location (hilar vs. other mediastinal).

Table 1. Characteristics of the study population (n = 97).*

Variable	No. (%)
Gender	
Male	62 (63.9%)
Female	35 (36.1%)
Age, y	
Mean ± standard deviation	66 ± 8.4
Range	42-84
Histology	
Adenocarcinoma	63 (64.9%)
Squamous cell carcinoma	17 (17.5%)
Others	17 (17.5%)
T stage (tumour-node-metastasis)	
1	27 (27.8%)
2	45 (46.4%)
3	15 (15.5%)
4	10 (10.3%)
Primary tumour SUV_{max}	
Mean ± standard deviation	9.64 ± 4.99
Range	1.07-21.5
EGFR status	
Wild type	28 (28.9%)
Mutated	20 (20.6%)
Unspecific	49 (50.5%)

Abbreviations: EGFR = epidermal growth factor receptor; SUV_{max} = maximum standardised uptake value.
* Data are shown as No. (%) or mean ± standard deviation, unless otherwise specified.

Table 2. Properties of lymph nodes (n = 467).

	No. (%)
Metastatic (histology proven)	59 (12.6%)
Benign (histology proven)	408 (87.4%)
Cases (n = 97)	
Cases with nodal metastases	38 (39.2%)
Cases without nodal metastases	59 (60.8%)
Hilar	170 (36.4%)
Other mediastinal	297 (63.6%)

RESULTS

Histology Findings

A total of 467 mediastinal/extramediastinal LNs from 97 patients (62 male, 35 female) of mean age 66 ± 8.4 years were included. The characteristics of the study population are summarised in Table 1. Adenocarcinoma was the most commonly reported histological finding. The properties of LNs are outlined in Table 2.

Positron Emission Tomography/Computed Tomography Performance

Figure 2 shows the ROC curves based on visual score, SUV_{max}, and nodal diameter. Their corresponding AUCs are listed in Table 3. The visual score achieved the highest AUC of 0.901 (95% confidence interval [CI] = 0.870-0.926), compared with 0.897 (95% CI = 0.866-0.923) for SUV_{max} and 0.804 (95% CI = 0.737-0.872) for nodal diameter, respectively. Whereas the difference in AUCs for visual score and SUV_{max} were not statistically significant (p = 0.796), their AUCs were significantly greater than those for nodal diameter (p = 0.0003). Figure 3 shows $\sqrt{(1-specificity)^2 + (1-sensitivity)^2}$ against visual score (lower X-axis) and SUV_{max} (upper X-axis). As mentioned above, the optimal diagnostic cut-off corresponds to the minimum of $\sqrt{(1-specificity)^2 + (1-sensitivity)^2}$. The cut-off for visual score was 3, implying that LNs with uptakes greater than or equal to that of liver should be suspicious for metastases. The optimal cut-off for SUV_{max} was 2.5 as demonstrated in Figure 3. Similar analysis for nodal diameter (not shown) gave a cut-off of 10 mm.

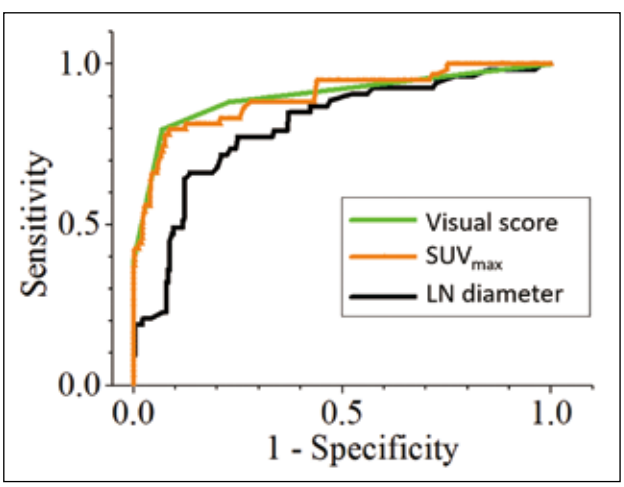

Figure 2. Receiver operating characteristics curves based on visual score, maximum standardised uptake value, and nodal diameter.
Abbreviations: LN = lymph node; SUV_{max} = maximum standardised uptake value.

Table 3. Diagnostic performance based on visual score, maximum standardised uptake value, and nodal diameter.

	Visual score (range)	SUV_{max} (range)	Nodal diameter (range)
Optimal cut-off	3	2.5	10 mm
AUC	0.901 (0.870-0.926)	0.897 (0.866-0.923)	0.804 (0.737-0.872)
p Value of AUC (compared with visual score)	-	0.796	0.0003
Sensitivity	0.810 (0.682-0.897)	0.810 (0.682-0.897)	0.660 (0.517-0.785)
Specificity	0.932 (0.901-0.953)	0.897 (0.868-0.924)	0.865 (0.813-0.906)
Accuracy	0.916 (0.880-0.953)	0.887 (0.845-0.929)	0.823 (0.778-0.867)
PPV	0.623 (0.507-0.733)	0.528 (0.420-0.633)	0.522 (0.398-0.644)
NPV	0.972 (0.949-0.985)	0.971 (0.950-0.984)	0.916 (0.869-0.948)

Abbreviations: AUC = area under the curve; NPV = negative predictive value; PPV = positive predictive value; SUV_{max} = maximum standardised uptake value.

Based on the cut-offs, the corresponding sensitivities, specificities, accuracies, positive predictive values (PPVs) and negative predictive values (NPVs) are evaluated in Table 3. Among SUV_{max}, visual score and nodal diameter, the visual score yielded the highest specificity (0.932, 95% CI = 0.901-0.953), accuracy (0.916, 95% CI = 0.880-0.953), PPV (0.623, 95% CI = 0.507-0.733), and NPV (0.972, 95% CI = 0.949-0.985). They were higher than those based on nodal diameter ($p = 0.0003$), although they had no statistically significant difference from the respective values of SUV_{max} ($p > 0.05$). On the other hand, the PET/CT achieved limited sensitivity based on nodal diameter (0.660, 95% CI = 0.517-0.785).

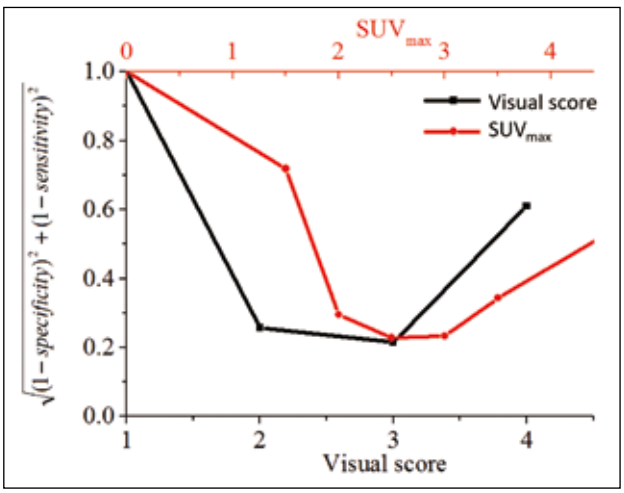

Figure 3. $\sqrt{(1-specificity)^2 + (1-sensitivity)^2}$ versus visual score (lower X-axis) and maximum standardised uptake value (upper X-axis).
Abbreviation: SUV_{max} = maximum standardised uptake value.

Subject-based staging rates are shown in Table 4. Based on visual interpretation, 77 subjects (79%) had correct nodal staging by visual score, whereas 12 subjects (12%) were false positive and eight (8%) were false negative. Based on SUV_{max}, 68 subjects (70%) had correct staging with 23 (24%) wrong upstaging and six (6%) wrong downstaging. Based on nodal diameter, 72 subjects (74%) had correct staging with 11 (11%) wrong upstaging and 14 (14%) wrong downstaging. The overall nodal staging performance achieved no significant difference between visual interpretation and nodal diameter in McNemar's test ($p = 0.190$), while that of SUV_{max} and nodal diameter had statistical significance ($p = 0.001$).

Table 4. Subject-based staging rates according to visual score, maximum standardised uptake value, and nodal diameter.

Subgroup	Visual score	SUV_{max}	Nodal diameter
Correct staging	79%	70%	74%
Wrong upstaging	12%	24%	11%
Wrong downstaging	8%	6%	14%

Abbreviation: SUV_{max} = maximum standardised uptake value.

Subgroup Analyses

Figure 4 shows the ROC curves of visual score according to T stage (T1-2 vs. T3-4), histology (adenocarcinoma vs. squamous cell carcinoma), EGFR status (wild type vs. mutated), primary tumour SUV_{max} (<10 vs. ≥10), and LN location (hilar vs. mediastinal). Their corresponding AUC values ranged from 0.838 to 0.961 (Table 6). For all subgroup analyses, the optimal cut-off of visual score was 3. To assess the significance of the difference between the AUCs, two-tailed tests were evaluated within the subgroups. The p values were > 0.05 for all subgroup analyses, except for histology, which had a p value of 0.0458.

DISCUSSION

Different radiological criteria have been proposed for nodal staging in NSCLC, including semiquantitative

SUV_{max},[10,11] qualitative visual interpretation,[13,14] and nodal diameter.[6,7] For visual interpretation, the current study focused on a five-point system[14] because of its convenient applicability (with reference to mediastinal blood pool and liver). We demonstrated good performance of the visual score. Subgroup analyses showed satisfactory AUCs in different T stages, histology, EGFR status, LN locations or primary SUV_{max}. There were no significant

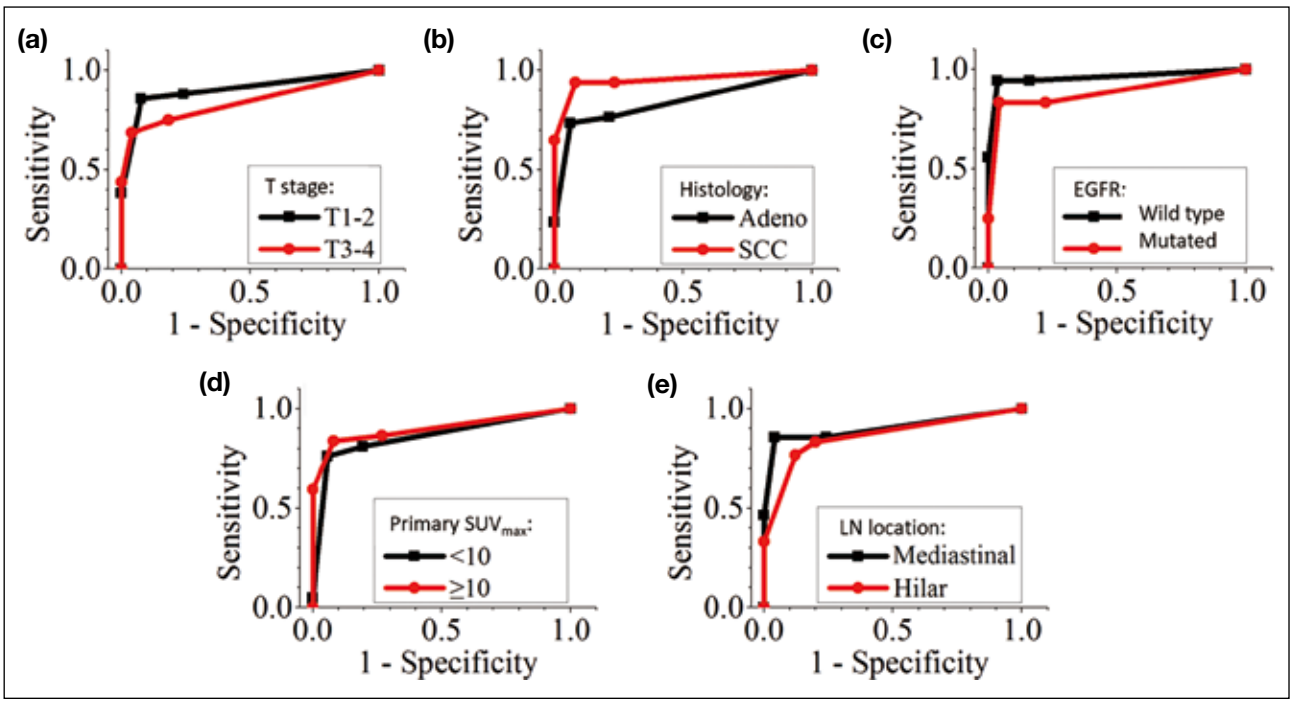

Figure 4. Subgroup receiver operating characteristics curves according to (a) T stage, (b) histology, (c) epidermal growth factor receptor status, (d) maximum standardised uptake value of primary tumour, and (e) lymph node location based on visual score.
Abbreviations: Adeno = adenocarcinoma; EGFR = epidermal growth factor receptor; LN = lymph node; SCC = squamous cell carcinoma; SUV_{max} = maximum standardised uptake value.

Table 5. Overall nodal staging performance with reference to histology.*

		Radiological nodal staging: 0 No. of cases based on		
		Visual score	SUV_{max}	Nodal diameter
Pathological nodal staging	0	49	39	50
	1	6	5	11
	2	2	1	3
		Radiological nodal staging: 1 No. of cases based on		
		Visual score	SUV_{max}	Nodal diameter
Pathological nodal staging	0	2	4	4
	1	10	10	5
	2	0	0	0
		Radiological nodal staging: 2 No. of cases based on		
		Visual score	SUV_{max}	Nodal diameter
Pathological nodal staging	0	8	16	5
	1	2	3	2
	2	18	19	17

Abbreviation: SUV_{max} = maximum standardised uptake value.
* Patients with N3 or N4 disease usually are not eligible for operation, therefore typically would not undergo histological lymph node staging.

Table 6. Subgroup areas under the curve according to T stage, histology, epidermal growth factor receptor status, primary maximum standardised uptake value, and nodal location.

Subgroup	AUC (95% confidence interval)
T stage	
1 & 2	0.904 (0.839-0.968)
3 & 4	0.84 (0.703-0.978)
p Value	0.370
Histology	
Adenocarcinoma	0.838 (0.745-0.93)
Squamous cell carcinoma	0.952 (0.877-1)
p Value	0.0458
EGFR status	
Wild type	0.961 (0.894-1)
Mutated	0.886 (0.747-1)
p Value	0.298
Primary SUV_{max}	
<10	0.86 (0.761-0.959)
≥10	0.9 (0.829-0.970)
p Value	0.523
Nodal location	
Hilar	0.863 (0.777-0.949)
Mediastinal	0.903 (0.818-0.989)
p Value	0.497

Abbreviations: AUC = area under the curve; EGFR = epidermal growth factor receptor; SUV_{max} = maximum standardised uptake value.

differences among the subgroups analyses, except for the histology, which had a borderline p value of 0.0458.

There were limited studies comparing the performance of visual score with SUV_{max} or nodal diameter.[13] Our study suggested that the visual interpretation achieved satisfactory AUC, specificity, accuracy, and NPVs. Such performance was statistically significant (p = 0.0003) compared with that of nodal diameter. While the cut-off for nodal diameter was 10 mm (axial plane), the smallest true positive LN identifiable by visual interpretation had a diameter of 7 mm with a SUV_{max} of 2.5 (corresponding primary tumour SUV_{max} = 11 and liver SUV_{mean} = 1.49). This example demonstrates the higher sensitivity of PET/CT to detect small malignant LNs compared with nodal diameter in CT alone. Although the visual score resulted in higher specificity, accuracy, PPV and NPV compared with SUV_{max} of 2.5, the differences were not statistically significant. A possible explanation is the similar cut-off magnitudes. A visual score with a cut-off of 3 corresponds to the liver's SUV_{mean} (range, 1.22-3.16). This is close to the SUV_{max} cut-off of 2.5 and therefore yields similar performance.

The limited sensitivity of 0.810 in visual interpretation was reviewed by examining the false negative cases.

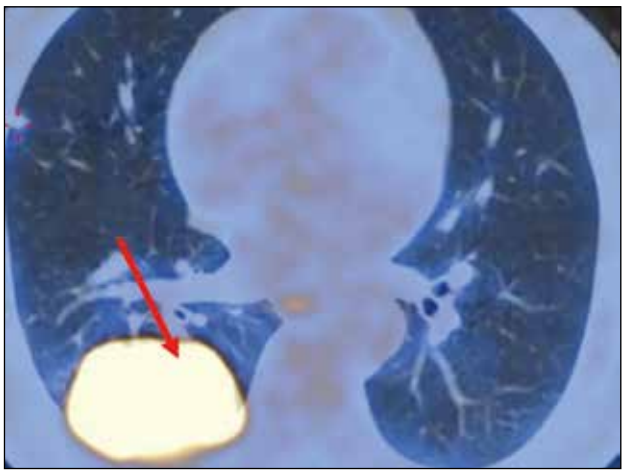

Figure 5. A large primary tumour can hinder the identification of an adjacent intrapulmonary lymph node (arrow), which was malignant in histology.

Among the eight false negative LNs, three (25%) may be explained by the limited PET/CT spatial resolution, as their pathology findings showed only a few clusters of tumour cells. Two cases (16.7%) may have been attributable to the close proximity of the primary tumour and LN. As illustrated in Figure 5, a large primary tumour limited the visualisation of the nearby intrapulmonary LN, which was proven to be malignant histologically. Whereas low ^{18}F-FDG uptake by the primary tumour may limit the identification of nodal metastases,[19] the 38 cases with nodal metastases all had ^{18}F-FDG–avid primaries. The least avid primary tumour with nodal metastasis had an SUV_{max} of 3.07, which was still distinguishable from the liver SUV_{mean} of 2.2. All nine (9.3%) cases with non–^{18}F-FDG avid primaries had no nodal metastases. We do not know what was behind the remaining seven false negative cases (58.3%).

Nodal staging is crucial for treatment of early-stage NSCLC.[4] For N1 and N2 disease treated with surgery, the adjuvant treatment is chemotherapy (N1) and sequential CRT (N2). For inoperable N2 disease, the primary treatment is CRT. Of the SUV_{max}, visual score and nodal diameter, the visual score achieved the most reliable overall staging, with an accuracy of 79% (Table 4). If a patient is mistakenly upstaged to N2 (10% subjects in the current report), his/her opportunity for curative surgery may be missed as they may receive CRT. If a patient is mistakenly downstaged from N2 disease (2% currently), his/her option for CRT instead of surgery may also be missed.

The cut-off of visual score in the current study was 3, implying that the LNs were suspicious for malignancy if their uptakes were greater than or equal to that of the liver (Figure 3). The identical cut-off of 3 was consistently observed in subgroup analyses (Figure 4). On the other hand, the cut-off in a previous study was >3,[14] implying malignancy if the uptake was >2 times the liver uptake or as elevated as that of the primary. The discrepancy of the two cut-offs may be due to different scanners, acquisition protocols, or reconstruction methods. Indeed, the same study suggested malignancy for a score of 3 as it was 3.3 times as likely to be malignant as a LN with a score of 2.[14]

In our study, the PPV based on visual interpretation was 0.623, which is less than the approximate value of 0.75 in the previous report.[14] This discrepancy may be explained by the fact that the lower the ratio of histologically malignant/total LNs, the lower the PPV. This ratio was 0.126 in the current study, which is lower than 0.194 in the previous report.[14]

The current study was limited by several factors. This was a retrospective study, thus it had no randomisation, and it was difficult to control confounders. The cases were all fit for histological workup and had no evidence of distant metastases. The study evaluated only 97 subjects and all were Chinese. The SUV depended on many factors, including scanner mode, acquisition protocol, and reconstruction method of the PET/CT.

CONCLUSION

PET/CT offers noninvasive preoperative nodal staging of NSCLC. A convenient visual interpretation is demonstrated to have diagnostic performance better than and similar to that of nodal diameter and SUV_{max}, respectively. The limited sensitivity can be attributed to the spatial resolution of PET/CT.

REFERENCES

1. Bray F, Ferlay J, Soerjomataram I, Siegel RL, Torre LA, Jemal A. Global cancer statistics 2018: GLOBOCAN estimates of incidence and mortality worldwide for 36 cancers in 185 countries. CA Cancer J Clin. 2018;68:394-424.
2. Edge SB, Compton CC. The American Joint Committee on Cancer: the 7th edition of the AJCC cancer staging manual and the future of TNM. Ann Surg Oncol. 2010;17:1471-4.
3. Detterbeck FC, Boffa DJ, Kim AW, Tanoue LT. The eighth edition lung cancer stage classification. Chest. 2017;151:193-203.
4. Ettinger DS, Wood DE, Aisner DL, Akerley W, Bauman J, Chirieac LR, et al. Non–small-cell lung cancer, version 5.2017, NCCN Clinical Practice Guidelines in Oncology. J Natl Compr Canc Netw. 2017;15:504-35.
5. Bacsa S, Czakó Z, Vezendi S. The complications of mediastinoscopy. Panminerva Med. 1974;16:402-6.
6. Bousema JE, Aarts MJ, Dijkgraaf MG, Annema JT, van den Broek FJ. Trends in mediastinal nodal staging and its impact on unforeseen N2 and survival in lung cancer. Eur Respir J. 2021;57:2001549.
7. Toloza EM, Harpole L, McCrory DC. Noninvasive staging of non–small-cell lung cancer: a review of the current evidence. Chest. 2003;123 (1 Suppl):137S-46S.
8. Schirrmeister H, Hetzel M, Buck A. Staging of non–small-cell lung cancer with integrated PET and CT. N Engl J Med. 2003;349:1188-90.
9. Antoch G, Stattaus J, Nemat AT, Marnitz S, Beyer T, Kuehl H, et al. Non–small-cell lung cancer: dual-modality PET/CT in preoperative staging. Radiology. 2003;229:526-33.
10. Bryant AS, Cerfolio RJ, Klemm KM, Ojha B. Maximum standard uptake value of mediastinal lymph nodes on integrated FDG-PET-CT predicts pathology in patients with non–small-cell lung cancer. Ann Thorac Surg. 2006;82:417-23.
11. Hellwig D, Graeter TP, Ukena D, Groeschel A, Sybrecht GW, Schaefers HJ, et al. ^{18}F-FDG PET for mediastinal staging of lung cancer: which SUV threshold makes sense? J Nucl Med. 2007;48:1761-6.
12. Hofman MS, Smeeton NC, Rankin SC, Nunan T, O'Doherty MJ. Observer variation in FDG PET-CT for staging of non–small-cell lung carcinoma. Eur J Nucl Med Mol Imaging. 2009;36:194-9.
13. Mathew B, Purandare NC, Pramesh CS, Karimundackal G, Jiwnani S, Agrawal A, et al. Improving accuracy of ^{18}F-fluorodeoxyglucose PET computed tomography to diagnose nodal involvement in non–small-cell lung cancer: utility of using various predictive models. Nucl Med Commun. 2021;42:535-44.
14. Rogasch JM, Apostolova I, Steffen IG, Steinkrüger FL, Genseke P, Riedel S, et al. Standardized visual reading of F18-FDG-PET in patients with non–small-cell lung cancer scheduled for preoperative thoracic lymph node staging. Eur J Radiol. 2016;85:1345-50.
15. Boellaard R. Standards for PET image acquisition and quantitative data analysis. J Nucl Med. 2009;50 Suppl 1:11S-20S.
16. Boellaard R, Krak NC, Hoekstra OS, Lammertsma AA. Effects of noise, image resolution, and ROI definition on the accuracy of standard uptake values: a simulation study. J Nucl Med. 2004;45:1519-27.
17. Boellaard R, Delgado-Bolton R, Oyen WJ, Giammarile F, Tatsch K, Eschner W, et al. FDG PET/CT: EANM procedure guidelines for tumour imaging: version 2.0. Eur J Nucl Med Mol Imaging. 2015;42:328-54.
18. Mountain CF, Dresler CM. Regional lymph node classification for lung cancer staging. Chest. 1997;111:1718-23.
19. Cloran FJ, Banks KP, Song WS, Kim Y, Bradley YC. Limitations of dual time point PET in the assessment of lung nodules with low FDG avidity. Lung Cancer. 2010;68:66-71.